International Journal of Advanced Research in Physical Science (IJARPS)
Volume 3, Issue 4, 2016, PP 13-20
ISSN 2349-7874 (Print) & ISSN 2349-7882 (Online)
www.arcjournals.org

Enhancement of the Magnetic Properties for Co-Mn-Zn Ferrites Nanoparticles using the Nonmagnetic Al^{3+}-Ions Substitution

M. M. Eltabey[*1, 2], A. M. Massoud[3, 4], Hany M. Mohamed[5, 6]

[1] Basic Engineering Science Department, Faculty of Engineering, Menoufiya University, Egypt
[2] Science Department, physics Division, Preparatory Year Deanship, Jazan University, Saudi Arabia
[3] Physics Department, Faculty of Science, Ain Shams University, Abbassia 11566, Cairo, Egypt
[4] Physics Department, Faculty of Science, Jazan University, Jazan, Saudi Arabia
[5] Chemistry Department, Faculty of Science, Al-Azhar University, Nasr City, Cairo 11884, Egypt
[6] Science Department, Chemistry Division, Preparatory Year Deanship, Jazan University, 82621, Jazan, Saudi Arabia
mohamed.eltabey@yahoo.com, amassouda1@yahoo.com, hmhamed@jazanu.edu.sa

Abstract: *Aluminum substituted cobalt manganese zinc ferrite nanoparticles $Co_{0.425}Mn_{0.425}Zn_{0.150}Al_xFe_{2-x}O_4$ (from x= 0.0 to 0.15 with step 0.025) have been synthesized by chemical co-precipitation route. X-ray diffraction (XRD) and infrared spectroscopy (FTIR) revealed that the obtained powders have a single phase of cubic spinel structure. The crystallite sizes calculated from XRD data have been confirmed using transmission electron microscopy (TEM) photographs showing that, the powders are consisting of nanosized grains with an average size around 19 nm independent on the Al-content. Magnetic hysteresis loops were traced at room temperature using VSM. It was found that due to the Al^{3+} - ions substitution, the values of saturation magnetization M_S for samples with $x \leq 0.075$ were improved. Whereas, both coercive field H_C and remnant magnetization M_r were decreased with increasing the Al-content. The obtained results were discussed in the light of non-collinear spin structure in the B-sites (Yafet-Kittle type of spin arrangement).*

Keywords: *Ferrites; IR spectra; Magnetic properties; Co-Mn-Zn ferrites; Al^{3+} -ions substitution.*

1. INTRODUCTION

Ferrites magnetic nanoparticles are attractive materials for they are widely used in electronic devices, such as transformers, recording heads, choke coils, noise filters, electromagnetic gadgets, data storage devices, etc.[1−3]. This wide range of applications comes from the very high d.c. resistivity compared to the metallic materials [4, 5]. Magnetic properties such as permeability, magnetization and coercive field are affected by the type of substitutant ions, microstructure and porosity [6]. Both Co-Zn and Mn-Zn ferrites are important from the point of view of the applications. Co-Zn ferrites have a considerable anisotropy and coercivity where Mn-Zn ferrites have a high initial permeability with a large magnetization [7, 8]. The combination between these two systems of ferrites has been synthesized and investigated by Y. Zhang et al. [9]. They reported that, Co^{2+}-ions in substituted Mn-Zn-ferrites ($Co_xMn_{1-x}Zn_{0.5}Fe_{1.5}O_4$) enhanced the values of magnetization for $x < 0.39$. Co-Zn ferrites nanoparticles were studied and it was found that the magnetic properties are optimized at Zn-concentration of 0.102 and Co- concentration of 0.898 [10, 11] where in case of Mn-Zn ferrites, the reported highest values of magnetic properties were found at Zn-concentration of 0.2 and Mn-concentration of 0.8 [5, 11]. The effect of substituting trivalent ions for iron has been studied [12-14]. Al^{3+}-ions substitution is used to tune the magnetic and electric properties of different ferrites was studied by many authors [8, 15-20]. They reported that, due to the substitution, there was a decrease in the values of saturation magnetization M_S, initial permeability μ_i, Curie temperature T_c, remanence ratio R, and coercive field H_c whereas the anisotropy field and electrical conductivity were increased. In previous work, a significant effect due to the Al^{3+}-ions substitution on magnetic and electric properties was reported in $Mn_{0.5}Ni_{0.1}Zn_{0.4}Al_xFe_{2-x}O_4$ ferrite system [10, 11]. In the present work, the combination between Co-Zn and Mn-Zn ferrites is studied in the system $Co_{0.425}Mn_{0.425}Zn_{0.150}Al_xFe_{2-x}O_4$ where the Zn-concentration (0.150) was selected to be the average value of that previously mentioned concentrations in references [5,10,11] to be near the optimum values of the magnetic properties. In addition, both Co and Mn- concentrations are equal with values of 0.425. The relatively

small concentrations of Al^{3+}-ions were selected according to previous reported work in which both microstructure and magnetic properties were investigated [4, 8, and 20].

2. EXPERIMENTAL

Cobalt Manganese Zinc nanoferrites substituted with varied quantities of Al^{3+}-ions ($Co_{0.425}$ $Mn_{0.425}$ $Zn_{0.150}$ Al_x Fe_{2-x} O_4; x = 0, 0.025, 0.050 , 0.075, 0.100, 0.125, 0.150) were synthesized via the chemical co-precipitation method using $CoSO_4$, $MnSO_4.1$ H_2O , $ZnSO_4$ $.7H_2O$, NaOH , $Al_2(SO_4)_3$ $.18H_2O$, and $FeCl_3$. Salts were mixed in the required stoichometric ratios in de-ionized water. Sodium hydroxide (NaOH) solution was then added dropwise, while stirring, until the measured pH value was 12. The mixture was continually stirred at 700 rpm for two hours while being heated at 80°C. A dark color was observed due to the formation of the ferrite particles. Particles were allowed to settle and the mixture was washed several times until the measured pH value was about 7. The powder samples were then allowed to dry at room temperature. X-ray diffraction (XRD) patterns were performed using the diffractometer of type Philips identify with $CuK_{\square}$ radiation ($\square$=1.5418Å). X-ray density d_x was calculated using the formula $d_x = (ZM)/(Na^3_{exp})$ [21, 22] where, M is the molecular weight, Z is the number of molecules per unit cell (Z = 8), N is Avogadro's number and a_{exp} is the experimental lattice parameter. The (311) reflection line in XRD pattern was used to calculate the average crystallite size D using the Debye-Scherrer equation, $D = (0.9\,\lambda)/(\beta\cos\theta)$ [1, 21] where, β is the full width at half maximum FWHM of the diffraction line in radian, and $\square$ is the corresponding diffraction angle in degree . The particle size and size distribution were observed by transmission electron microscope (TEM). The grain micrographs were obtained by low vacuum TEM JEOL (JEM-1400 TEM). FTIR spectra were carried out (using Perkin Elmer spectro-photometer) in the wavenumbers range 150-650 cm^{-1}. Hysteresis loops were obtained at room temperature in a magnetizing field H (Oe) ranged from -1500 to 1500 Oe using the Lake Shore vibrating sample magnetometer (VSM) model 7410. Saturation magnetization M_s (emu/g), remnant magnetization M_r (emu/g) coercive field H_c (Oe) , energy loss ε (erg/g) are determined automatically.

3. RESULTS AND DISCUSSION

3.1. Structural Properties

3.1.1. X-Ray Analysis

XRD patterns in Fig.1 indicate that all samples are formed in cubic single spinel phase. The values of d-spacing are calculated according to Bragg's law and hence the average experimental lattice parameters a_{exp} (Å) are calculated. The variation of a_{exp} with the Al- concentration is plotted in Fig. 2. It is clear that as the Al- concentration increases the experimental lattice parameter decreases almost linearly obeying Vegard's law. Similar behavior was observed in Al- substituted Ni-Cu-Zn[4], Mn-Zn-Ni ferrites [20].

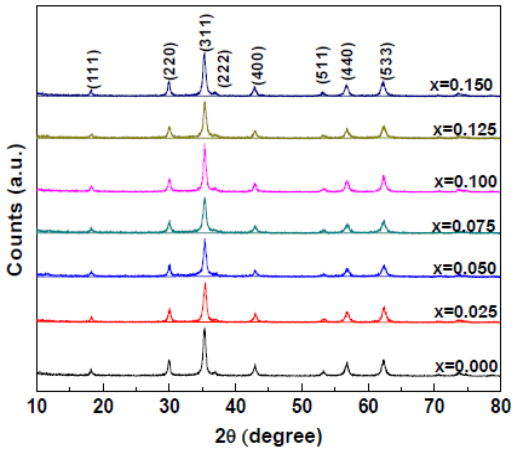

Fig1. *X-ray diffraction pattern of the system* $Co_{0.425}Mn_{0.425}Zn_{0.150}Al_xFe_{2-x}O_4$

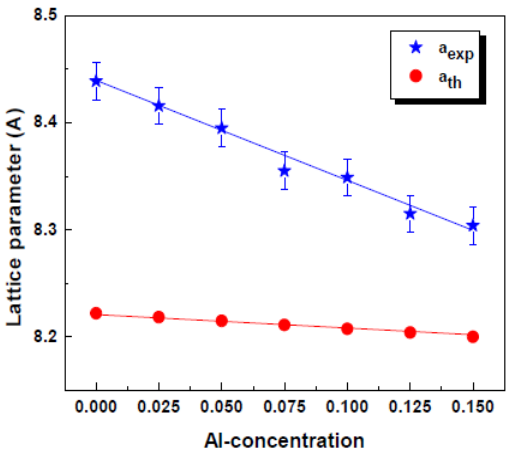

Fig2. *Change of experimental and theoretical lattice parameters wit h Al-concentration*

The linearity in the composition dependence between the experimental lattice parameter and the Al-concentration indicates also that the Al is completely inverses spinel [23] as it will be discussed in details in the IR section. The decrease in experimental lattice parameter could be explained on the

basis of the ionic radii due to the replacement of ions with larger ionic radius of Fe^{3+} (0.645 Å) by the smaller ones of Al^{3+} (0.535 Å). The composition dependence of crystallite size D is listed in table1. Values of D reveal that there is no considerable change in the crystallite size due to Al^{3+}-ions substitution. This could be attributed to the tiny amounts of Al^{3+}-ions that are doped just to tune the magnetic properties of the Co-Mn-Zn ferrites. The theoretical lattice parameters a_{th}(Å) were calculated according to the following cation distribution:

$$(Mn^{2+}_{0.34}Zn^{2+}_{0.15}Co^{2+}_{0.17}Fe^{3+}_{0.34})_A\ [Mn^{2+}_{0.085}Co^{2+}_{0.255}Al^{3+}_{x}Fe^{3+}_{(1.66-x-t)}Fe^{2+}_{t}]_B \quad (1)$$

which is assumed in the light of the following bases:

1. For manganese, 80% of Mn ions occupy the tetrahedral positions (A-sites) and the remaining, 20%, occupy the octahedral positions (B-sites) [24].
2. Zn ions prefer to occupy the tetrahedral sites and 60% of Co ions occupy the octahedral sites and the remaining 40% occupy the tetrahedral positions [25].
3. Concerning Al^{3+} ions, several authors [26-32] reported that it is distributed between the tetrahedral and octahedral sites. Meanwhile, other authors [33-36] showed that the Al^{3+}-ions occupy completely the octahedral sites. In the current work, IR spectroscopic analysis supported that Al^{3+}-ions are located in the B-sites as will be shown later.

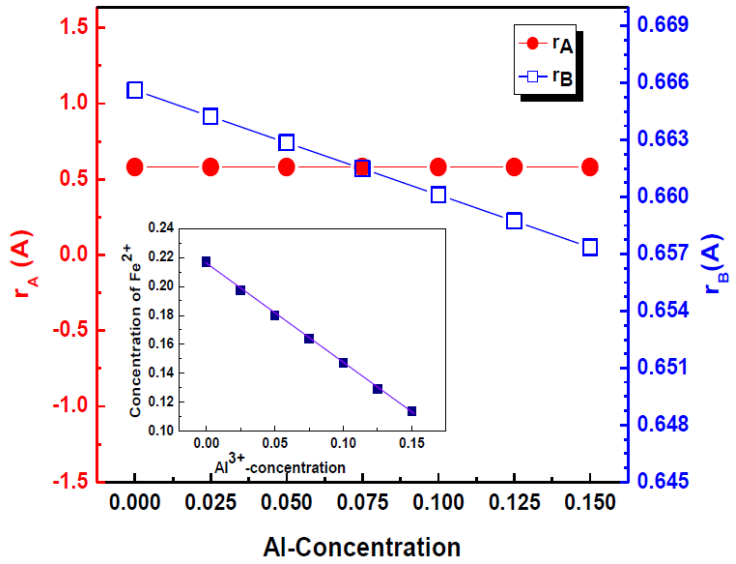

Fig3. *Variation of r_A, r_B and Fe^{2+}-ions concentration (inset) with Al-concentration*

Divalent iron Fe^{2+}-ions are taken into consideration since they are formed according to the oxidation process as well as to the metal-metal charge transfer transition [37, 38]. Consequently, the ionic radius for each site is calculated according to the following equations:

$$r_A = 0.34\ r_{Mn^{2+}} + 0.15\ r_{Zn^{2+}} + 0.17 r_{Co^{2+}} + 0.34\ r_{Fe^{3+}} \quad (2)$$

$$r_B = \frac{1}{2}[0.085\ r_{Mn^{2+}} + 0.255\ r_{Co^{2+}} + x r_{Al^{3+}} + (1.66 - x - t) r_{Fe^{3+}} + t r_{Fe^{2+}}] \quad (3)$$

where, $r_{Mn^{2+}}, r_{Zn^{2+}}, r_{Fe^{3+}}, r_{Co^{2+}}, r_{Al^{3+}}, r_{Fe^{2+}}$ are the ionic radii of manganese, zinc, trivalent iron, cobalt , aluminum ion and divalent iron ions respectively. The used values of the ionic radii are dependent on the coordination number [39]. Theoretical lattice parameters a_{th} are calculated according to equation (4) where r_B is calculated after omitting the presence of Fe^{2+}-ions [8]:

$$a_{th} = \frac{8}{3\sqrt{3}}[(r_A + R_O) + \sqrt{3}(r_B + R_O)] \quad (4)$$

Where, R_O is the radius of the oxygen ion (1.32 Å). Theoretical and experimental lattice parameters as a function of the Al-content are plotted in Fig 2. It is clear that both parameters are decreasing with Al-concentration and the difference between them is decreasing as the Al-concentration increases. This behavior could be attributed to the existence of Fe^{2+}-ions. The concentration of Fe^{2+}-ions (t) is calculated from the coincidence between the values of theoretical and experimental lattice parameters.

The composition dependence of Fe^{2+}-ions concentration is represented as an inset in Fig.3 showing that the values of t is decreasing with increasing the Al-content. X-ray densities are calculated and listed in Table 1. As Al^{3+} concentration increases, the x-ray density goes up. This could be attributed to the decrease of a_{exp} with Al-content. It is clear that the effect of lattice parameter dominates that of molecular weight which is smaller for subistitutant Al^{3+}-ions compared to that of Fe^{3+}-ions.

3.1.2. FT IR Spectra Analysis

Figure 4 shows the FT IR spectra for the samples with x= 0, 0.05, 0.1 and 0.15. It is obvious that there exist three fundamental bands $\{\nu_1, \nu_2, \nu_3\}$ confirming that present system is a cubic inverse spinel [20]. It has been reported that the first two IR fundamental bands are due to tetrahedral and octahedral complexes, while the third one is due to that lattice vibrations [40]. Positions of the IR bands of the studied samples were recorded automatically and they are given in table 1. The high frequency band ν_1 (510 -583 cm^{-1}) is attributed to the vibration of the iron ions in the tetrahedral positions. The second band ν_2 (311-495 cm^{-1}) is associated to the divalent octahedral metal ions and oxygen complexes. Finally, the third vibrational band (less than 300 cm^{-1}) is attributed to the lattice vibrational frequency [41].

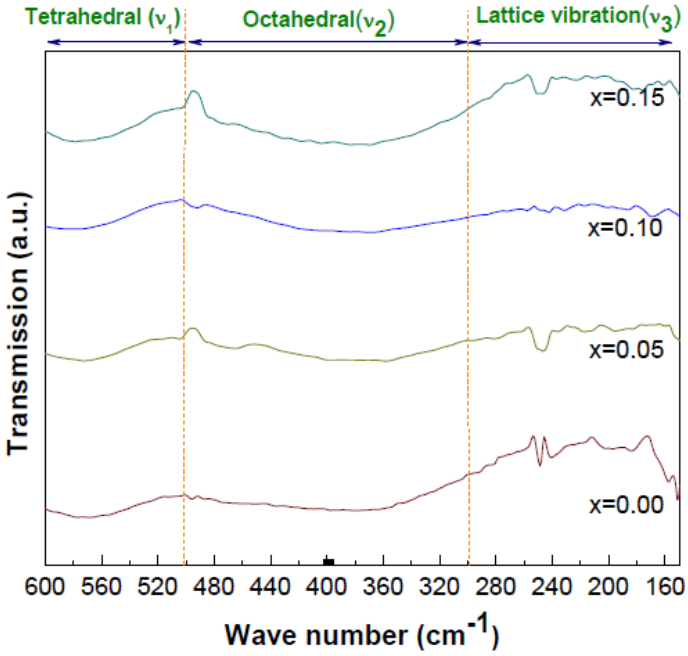

Fig4. *FTIR spectra of the system* $Co_{0.425}\,Mn_{0.425}Zn_{0.150}\,Al_x\,Fe_{2-x}\,O_4$

Table1. *Variation of crystallite size (D), X-ray density (d_x) , and FTIR absorption bands with Al- content (x)*

X	D(nm)	d_x ($g.cm^{-3}$)	FTIR absorption bands		
			$\nu_1(cm^{-1})$	$\nu_2(cm^{-1})$	$\nu_3(cm^{-1})$
0	20.15	5.2190	576, 511	495, 378	248 ,240, 196, 184, 157
0.025	19.87	5.4260	---	---	---
0.050	19.17	5.6425	574, 512	467, 389, 466	257, 240, 229, 220, 202, 188, 179, 161
0.075	19.03	5.6812	---	---	---
0.100	17.77	5.9435	571, 510	496, 487, 361, 345, 336, 323, 311	297, 291, 268, 242, 207, 197, 188, 172
0.125	17.39	5.9123	---	---	---
0.150	17.73	5.9834	575, 511	409, 376	257, 240, 228, 215, 182, 173

It is clear that, no considerable change is observed in the values of ν_1 with increasing the Al-content. This result supports the assumption that Al^{3+}-ions totally occupy the octahedral sites and explains the constancy behavior of r_A with Al-content as shown in Fig.3. The second band shows non trendy behavior in frequency positions with increasing the Al-concentration. This is could be due to the existence of many ions inside the B-sites as well as to the continuous charge transfer between the Fe^{3+}

and Co^{2+} - ions forming Fe^{2+} and Co^{3+} - ions [39]. That transfer leads to change in the ionic radii which cause the noticeable fluctuation in the wavenumbers of the octahedral absorption bands. This fluctuation in the B-site bands due to the Al^{3+}-ions substitution emphasizes the presence of Al^{3+}- ions in B-sites only in such a ferrite system. According to the above discussion, the decrease of lattice parameter with increasing Al-content could be attributed to the decrease of r_B with increasing Al-concentration as shown in Fig.3 supporting the assumed cation distribution.

3.1.3. TEM Micrographs

Transmission electron micrographs, TEM micrographs, were performed for samples with x=0, 0.05, 0.1 and 0.15 as an example. Fig. 5 (a) shows the nanosized particles of the unsubstituted sample (x = 0). The particle size distribution is represented by the histogram shown in Fig. 5 (b). The average value of particle size which is obtained from TEM micrograph was found to be close to that calculated using Debye-Scherrer equation.

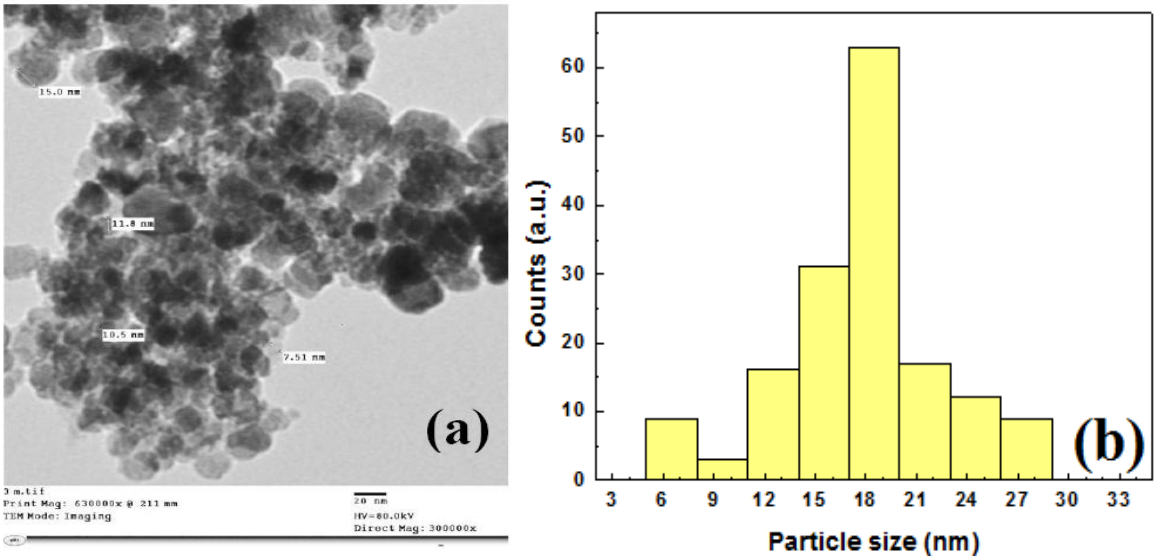

Fig5. *TEM micrograph for sample with x=0 (a) and its particle size distribution (b).*

Fig. 6 (a-d) shows the TEM micrographs for the four selected samples. One can note that Al-substitution in this system of ferrite has no considerable effect on the average particle size. This could be attributed to the few amount of Al^{3+}-ions which are used just to modify the magnetic properties.

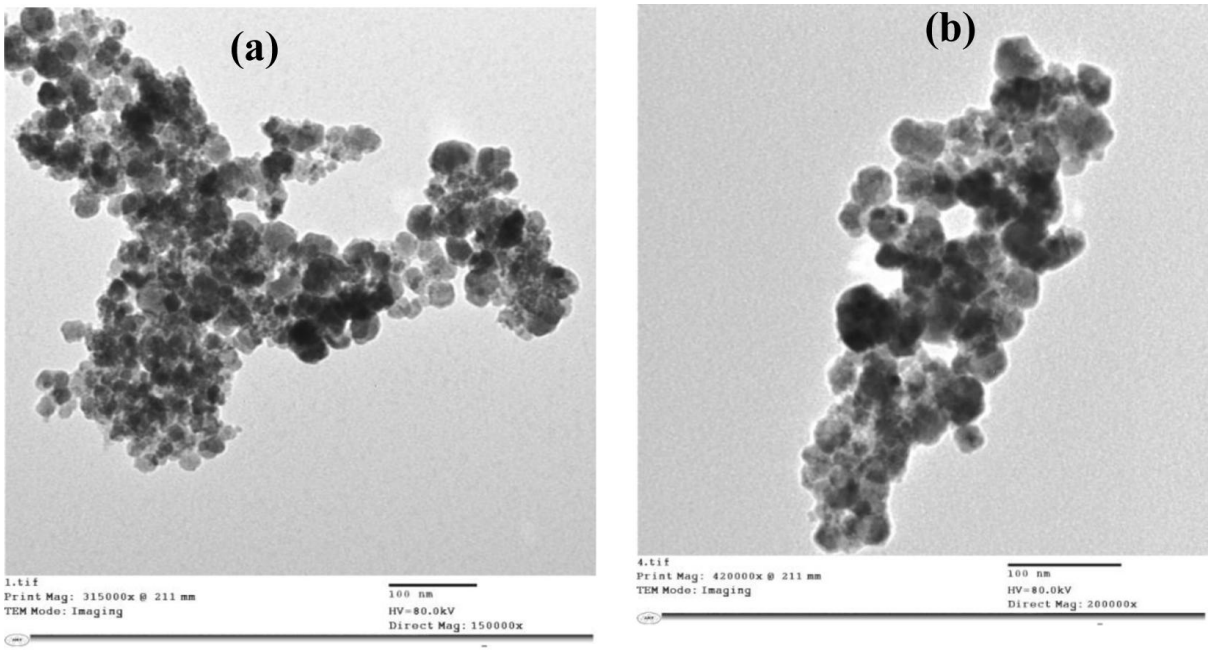

x = 0 **x = 0.05**

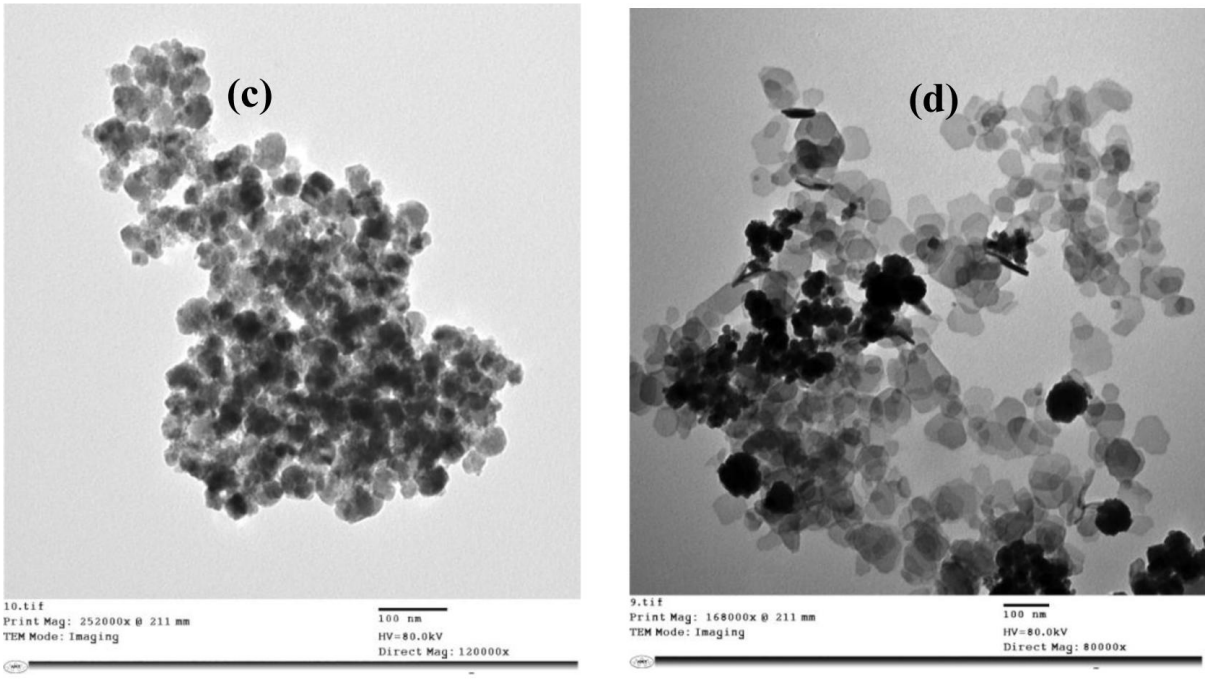

Fig6. *TEM micrographs of the system $Co_{0.425}$ $Mn_{0.425}Zn_{0.150}$ Al_x Fe_{2-x} O_4 ; (a) x = 0, (b) x = 0.05, (c) x = 0.1 and (d) x = 0.15*

3.2. Magnetic Properties

Hysteresis loops at room temperature for all investigated samples are shown in Fig. 7 where the values of magnetization scale on the graph for each loop ranges from -50 to +50 (emu/g). One can note that as the Al-concentration increases, the hysteresis loops become narrower. Variation of saturation magnetization M_s (emu/g) with the Al-concentration is represented in Fig. 8.

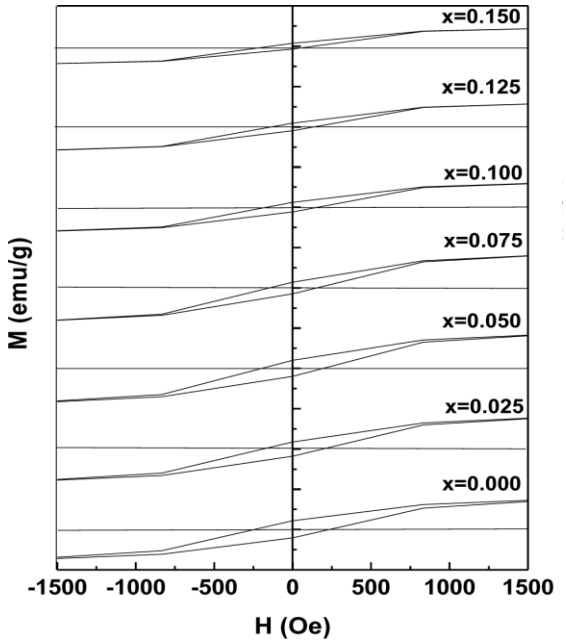

Fig7. *Hysteresis loops of the system $Co_{0.425}$ $Mn_{0.425}Zn_{0.150}$ Al_x Fe_{2-x} O_4 [M-scale is ranging from -50 to 50 (emu/g) for each sample]*

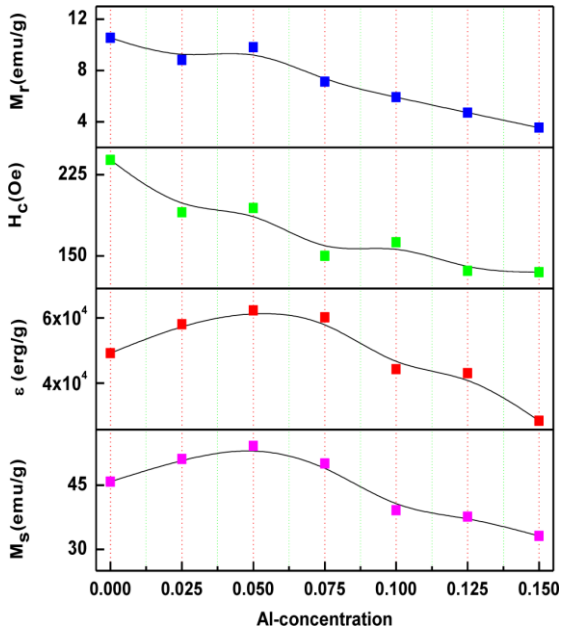

Fig8. *Saturation magnetization M_s, Remnant magnetization M_r, coercive filed H_c and energy loss as functions if Al-content for the system $Co_{0.425}$ $Mn_{0.425}Zn_{0.150}$ Al_x Fe_{2-x} O_4*

It is clear that as Al-content increases, the values of M_s become almost higher than that of the unsubstituted sample up to x = 0.075 with maximum value at x = 0.05 with percentage increase equal 10 %. For x > 0.075, the values of M_s tend to decrease. This behavior could be explained on the basis of non-collinear spin structure in the B-sites. Spin canting effects in B-sublallice is known as Yafet-

Kittle type of spin arrangement due to the presence of canting angle (α_{yk}) between moments in the B-sites [42]. In the light of that arrangement, the total magnetization M could be expressed as [20]:

$$M=M_B \cos \alpha_{yk} - M_A, \quad (5)$$

where M_A and M_B are the magnetic moments of A and B- sites respectively. Using the assumed cation distribution and taking the values of the magnetic moments of Fe^{3+}, Zn^{2+}, Al^{3+}, Co^{2+} , Mn^{2+} and Fe^{2+} as 5, 0, 0, 3 5 and 4 μ_B respectively, the total magnetic moment could be written as;

$$M = (9.49-5x-t) \cos \alpha_{yk} - 3.91 \quad (6)$$

From equation (6), the increase in M with x up to 0.075 could be attributed to the increase of cos α_{yk} , i.e., a decrease in the values of the angle α_{yk} . For x > 0.075 , i.e., further replacement of Fe^{3+}-ions by non-magnetic Al^{3+}-ions in B sites leads to a decrease of the magnetization and hence the total magnetization should decrease as found experimentally. This means , after improving parallelism between moments at x=0.05, the further replacement of Fe^{3+}-ions by non-magnetic Al^{3+}-ions in B-site leads to a decrease in the value of M_B and hence the magnetization should decrease. The composition dependence of hysteresis energy loss, which is related to the area of the loop, is represented in Fig.8. Its behavior is nearly similar to that of magnetization. It is well known that, in magnetic materials, the magnetic energy loss depends strongly on the values of saturation magnetization, remnant magnetization and coercive field [43] which explains the coincidence between the behaviors of magnetization and energy loss. Variation of both coercive field H_c and remanence M_r with the Al-content is illustrated in Fig.8. It is obvious that both H_c and M_r are decreasing with increasing the Al-content. Behavior of H_c with the Al-content could be explained in light of the Brown's relation where H_c is related to the saturation magnetization as follows [44]:

$$H_c \geq \frac{2k}{\mu_o M_s} \quad (7)$$

where k is the anisotropy constant. It is known that the anisotropy field in ferrites arises mainly from the existence of Fe^{2+} -ions [45]. As shown before, Fe^{2+} contents decreases with increasing Al-concentration. This leads to the decrease of the anisotropy constant. Meanwhile, both the increase of M_s and the decrease of k (up to x = 0.075) forces the values of H_c to decrease as the Al-concentration increase. For x > 0.075 the decrease in H_c shows that the effect of k is the predominant. It is known that, the values of remnant magnetization is related directly to the magnitude of the anisotropy constant [46] which explains the decrease of M_r with the increasing Al-content due to the decrease of anisotropy.

4. CONCLUSION

A spinel cubic single phase of $Co_{0.425}\ Mn_{0.425}\ Zn_{0.150}\ Al_x\ Fe_{2-x}\ O_4$ ferrite (x = 0 - 0.15 with step 0.025) has been prepared using the chemical co-precipitation technique. As a result of Al-substitution, it was found that:

1. The values of lattice parameter were decreased whereas both the calculated crystallite size and average particle size obtained from TEM micrographs showed no considerable change.
2. Saturation magnetization was enhanced up to x = 0.075 with an increase of 10% for the sample with x = 0.05
3. Both coercive field and remnant magnetization decreased with increasing Al-content.

ACKNOWLEDGMENT

The authors would like to acknowledge the Research Deanship, Jazan University for the financial support of this work with grant number 286.

REFERENCES

[1] M Ben Ali , K El Maalam, H El Moussaoui, O Mounkachi, M Hamedoun, R Masrour, E K Hlil, A Benyoussef, *J. Magn. Magn. Mater.* 398 20 (2016)

[2] Mohamed Eltabey, Ebrahim Hassan, Ismail Abd Elrahim Ali, *Am. J. Appl. Sci*. 11(1) 109 (2014)

[3] Humaira Anwar , Asghari Maqsood, I H Gul, *J. Alloy Compd*. 626 410 (2015)

[4] M M Eltabey, K M El shokrofy, S A Gharbia, *J. Alloy Compd.* 509 2473(2011)

[5] Hassan Hejase, Saleh S. Hayek, Shahnaz Qadri, and Yousef Haik, *J. Magn. Magn. Mater*. 324 3620 (2012)
[6] G C Jain, B K Das, R S Khanduja, S C Gupta, *J. Mater. Sci.* 11 1335 (1976)
[7] Ibrahim Sharifi, H Shokrollahi, *J. Magn. Magn. Mater*. 334 36 (2013)
[8] A A Sattar, H M El-Sayed, M M El-Tabey, *J. Mater. Sci.* 40 (18) 4873 (2005)
[9] Youxian Zhang, Jiaona Fan, Qian Li, Yongtao An, Chuanhui Liang, and Xueqin An, Synth. *React Inorg Me.* 40 556 (2010)
[10] Ritu Rani, S K Sharma, K R Pirita, M Knobel, Sangeeta Thakur, M Singh, *Cer. Int.* 38 2389 (2012)
[11] R Arulmurugan, B Jeyadevan, G Vaidyanathan, S Sendhilnathan, *J. Magn. Magn. Mater*. 288 470 (2005)
[12] K P Belove, L A Antoshina, A S Moreosyan, *Fiz. Tverd. Tela*+ 25 2791 (1983)
[13] M A Ahmed, A Tawfik, M K El-Nimr, A A El-Hasab, *J. Mater. Sci*. 10 549 (1991)
[14] A M Samy, H M El-Sayed, A A Sattar, *J. Phys. Stat. Sol. (A),* 200 401 (2003)
[15] A G Bhosale, B K Chougule, *Mater. Chem. Phys.* 97 273 (2006)
[16] G J Baldha, K G Saija, K B Modi, H H Joshi, R G Kulkarni, *J. Mater. Lett.* 53 233 (2002)
[17] Y -P Fu, S Tsao, C -T Hu, Y -D Yao, *J. Alloy Compd*. 395 272 (2005)
[18] A M Sankpal, S S Suryawanshi, S V Kakatkar, G G Tengshe, R S Patil, N D Chaudhari, S R Sawant, *J. Magn. Magn. Mater.* 186 349 (1998)
[19] U V Chhaya, B S Trivedi, R G Kulkarni, *J. Phys. B* 262 5 (1999)
[20] A A Sattar, H M El-Sayed, K M El-Shokrofy, M M El-Tabey, *J. Appl. Sci.* 5 (1) 162 (2005)
[21] B D Cullity *Elements of X-ray Diffraction* (Addison Wesley pub Co. Inc.) p 99 (1956)
[22] H M Zaki , S H Al-Heniti, T A Elmosalami, *J. Alloy. Compd.* 633 104 (2015)
[23] U V Chhaya, R G Kulkarni, *Mater. Lett.* 39 91 (1999)
[24] F Petil , M Lenglet, *Solid State Commun.* 86 67 (1993)
[25] Sonal Singhal, J Singh, S K Barthwal, K Chandra, *J. Solid State Chem.* 178 3183 (2005)
[26] A M Abo El Ata, S M Attia and T M Meaz, *J. Solid State Sci*. 6 61 (2004)
[27] V Urvi, S Bimal, R. Kulkarni, *Physica B.* 262 5 (1999)
[28] Seo Wook, Young Lee, Kwang Pyo and Sungtto, *J. Korean Phy. Soc.* 34 378 (1999)
[29] R G Kulkarni, Bimal S Trivedi, H H Joshi, G J Baldha , *J. Mag. Mater.* 159 375 (1996)
[30] T Jung, D Park, S Kwon, *IEEE T Magn.* 31 3979 (1995)
[31] A Ashfaq, *J. Mater. Sci.* 27 4120 (1992)
[32] M Rosenberg, P Deppe and H Janssen, *J. Appl. Phys.* 57 3740 (1985)
[33] P Chandra, *J. Mater. Sci. Lett.* 6 651 (1987)
[34] S S Suryawanshi, V V Deshpande, U B Deshmukh, S. M Kabur, N D Chaudhari, S R Sawant, *Mater. Chem. Phys.* 59 199 (1999)
[35] A M Sankpal, S V Kakatkar, N D Chaudhari, R S Patil, S R Sawant, S S Suryavanshi, Initial permeability studies on Al^{3+} and Cr^{3+} substituted Ni-Zn ferrites, *J. Mater. Sci.-Mater. El.* 9 173 (1998)
[36] N Sparvieri, F Cattarin , *Mater. Chem. Phys.* 25 167 (1990)
[37] A Angermann, J Töpfer, K L da Silva, K D Becker, *J. Alloy. Compd.* 508 433 (2010)
[38] I H Gula, A Maqsooda, M Naeemb, M Naeem Ashiqc , *J. Alloy. Compd.* 507 201 (2010)
[39] R D Shannon, *Acta Cryst. A* 32 751 (1976)
[40] K Mohan, and Y C Venudhar, *J. Mater. Sci. Lett.* 18 13 (1999)
[41] M A Ahmed, E Ateia and S I El-dek, *Vib Spectrosc* 30 69 (2002)
[42] J Smit, *Magnetic Properties of Materials* (Mcgraw Hill Book Co.) p 89 (1971)
[43] P A Shaikh, R C Kambale, A V Rao, Y D Kolekar, *J. Alloy. Compd.* 492 590 (2010)
[44] J M D Coey *Rare-earth Permanent Magnetism* (John Wiley and Sons, New York) p 220 (1996)
[45] S Chikazumi and S Charap *Physics of Magnetism* (John Wiley and Sons, Inc., New York, London, Sydney) p 153 (1964)
[46] M M El-Okr, M A Salem, M S Salim, R M El-Okr, M Ashoush, H M Talaat, *J. Magn. Magn. Mater.* 323 920 (2011)